Abstract

The cellular interior is crowded, with macromolecules occupying from 10% to 40% of the volume.[1] Under these conditions, proteins experience hard-core repulsions and chemical interactions with cytoplasmic components.[2,3] Hard-core repulsions stabilize globular proteins, whereas chemical interactions can be either repulsive and stabilizing, or attractive and destabilizing.[2,3] Several studies have considered crowding effects on globular protein stability[4–7], but there are few such studies on protein-protein interactions. We used ^{19}F NMR to quantify the effects (298 K, pH 7.5) of macromolecular cosolutes on a variant of the B1 domain of protein G (GB1) that forms a domain-swapped homodimer.[8] At a concentration of 200 g/L, the monomer of the synthetic polymer polyethylene glycol (PEG) destabilizes the dimer by 0.30 kcal/mol, while at the same concentration, 3.3 kDa-, 8 kDa- and 20 kDa- PEG stabilize the dimer by 0.08, 0.39 and 0.4 kcal/mol, respectively. These data indicate a stabilizing, but saturable, macromolecular effect. We also showed that the physiologically-relevant cosolutes bovine serum albumin (BSA) and lysozyme have opposite effects; the former (at 100 g/L) stabilizes the dimer by 0.51 kcal/mol, and the latter (at 50 g/L) destabilizes the dimer by 0.12 kcal/mol. These results can be explained by the differences in charge. BSA has the same charge as GB1, resulting in stabilizing repulsions. Lysozyme and GB1 have complementary charges, resulting in destabilizing attractions. The differing effects of PEG and the protein cosolutes indicate that synthetic polymers are poor mimics of the cellular interior because they do not account for chemical interactions found in cells.

Background: Proteins are mostly studied in dilute buffer, where the concentration of macromolecules is <10 g/L. However, the cytoplasm is highly crowded milieu where the concentration of macromolecules can exceed 300 g/L.[9] At these concentrations, the effects of cosolutes on protein stability can no longer be ignored.[2] Although such interactions can be described as weak and transient, they play a major role in protein function and stability.[4,7]

These transient cosolute-protein interactions can be fall into one of two categories: hard-core repulsions and chemical interactions.[2] Hard-core repulsions are steric interactions that arise from a decrease in the available volume.[2] Chemical interactions can be briefly defined as nonspecific interactions between the protein and molecules in solution (hydrogen bonding, polar/nonpolar interactions, etc.).[2]

Large polymers, such as polyethylene glycol (PEG) and Ficoll, have often been used to simulate these high concentration conditions. These solutes cause for the weak transient interactions to manifest themselves in the form of hard-core repulsions and chemical interactions.[2] Hard-core repulsions are steric interactions that arise from a decrease in the available volume.[3] A decrease in volume pushes a single globular protein to a more compact state.[2]

Then, chemical interactions may be either repulsive or attractive. These arise from transient interactions between the protein of interest and the cosolutes in solution.[2] If they are favorable (hydrogen bonding, polar/nonpolar interactions, etc.), then they lead to the globular protein favoring a more open state (opening yields more points of contact for favorable interactions).[2] If they are unfavorable (such as charge repulsions), the

globular protein becomes more compact (closing yields less points of contact for unfavorable interactions).[2]

However, all of these observations are made for single globular proteins. Although it is easier to think of cells as a mass of globular proteins acting in tandem, it is incorrect to say that they act alone. There are a myriad of protein-protein interactions (PPIs) that are involved in everything from metabolism, to cellular structure, to even disease.[10–12]

A variant (L5V;F30V;Y33F;A34F) of the monomeric B1 domain of protein G (GB1) will serve as the test protein for understanding the effects of crowding on PPIs (figure 1). The mutations destabilize the monomeric GB1 protein.[8] However, the variant undergoes intermolecular domain swapping through exchanging second β-hairpins each, forming a thermodynamically favorable structure compared to the destabilized monomer.[8]

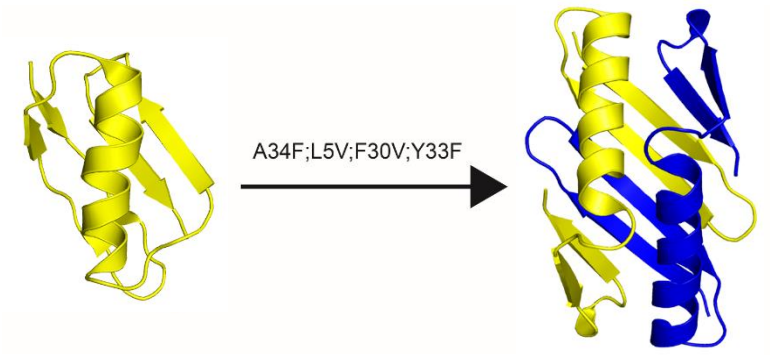

Figure 1: Wild-type GB1 (left) and the domain-swapped homodimer variant (right).

GB1 contains one tryptophan, which can be fluorine-labeled using the metabolic precursor 5-fluoroindole, allowing ^{19}F nuclear magnetic resonance (NMR) to be used to observe both the dimer and monomer states. ^{19}F is NMR–active, 100% abundant, rarely found in biological

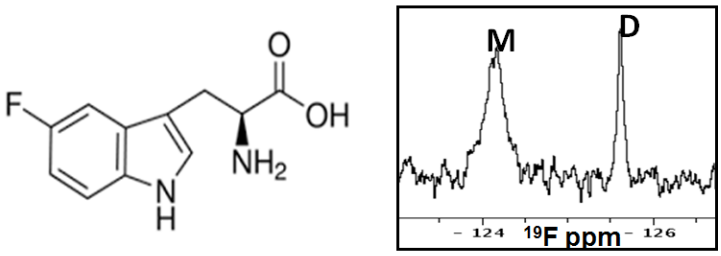

Figure 2: The addition of the 5-fluoroindole (left) to the media allows us to monitor the monomer and dimer states by ^{19}F NMR (right).

systems, has 83% of the NMR sensitivity of proton, and a chemical shift highly sensitive to environment.[13,14]

The physical behavior of polymers vary based on concentration, and these shifts in behavior have been shown have an effect on proteins.[4] Polymers exist in several different states based on concentration, two of which are dilute and semi-dilute.[15] In the dilute state, the individual polymer molecules can be thought of as individual molecules that are not interacting. The semi-dilute state is much different, where the polymer molecules stop acting like individual spheres and begin to interact, forming a mesh.[15] The concentration at which this transition from the dilute to the semi-dilute regime occurs is called the overlap concentration (*c**).[15] This behavior is summarized in Figure 3. These polymer effects are governed by many factors, one of which is their chain length. To better understand the effects of macromolecular polymerization on dimerization, we will study the effects of long-chain polymers on dimer stability.

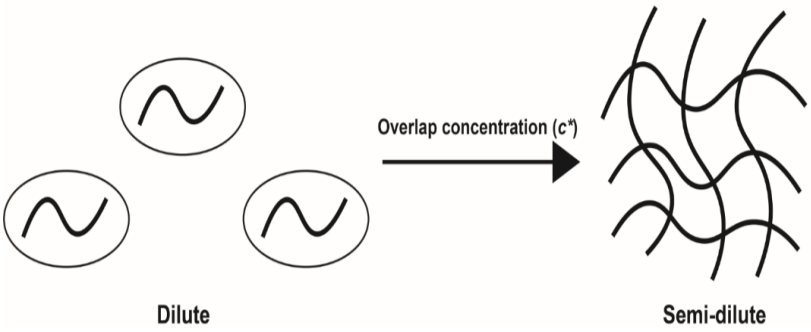

Figure 3: Polymers can be approximated as individual molecules before reaching their overlap concentration, c*.

Results

Hard core repulsions, monomers of polymers. The polymers 8 kDa PEG and 70 kDa Ficoll were used to probe hard core-repulsions. Solutions were made to a final concentration of 200 g/L and 300 g/L of 8 kDa PEG and 70 kDa Ficoll, respectively. Ethylene glycol (the monomer of PEG) and sucrose (the monomer of Ficoll) were used at the same concentration as their polymer counterparts. Buffer containing 300 g/L 70 kDa Ficoll yielded a $K_{D\rightarrow M}$ of 27 ± 2 μM, and buffer containing 200 g/L 8 kDa PEG yielding a $K_{D\rightarrow M}$ of 46 ± 3 μM. Buffer containing 200 g/L ethylene glycol resulted in a $K_{D\rightarrow M}$ of 153 ± 12 μM, while buffer containing 300 g/L sucrose yielding a $K_{D\rightarrow M}$ of 58 ± 4 μM. These data were used to calculate the $\Delta\Delta G'^{o}_{D\rightarrow M}$, and uncertainties were calculated as standard deviation of the mean from triplicate analysis. These results are summarized in figure 4.

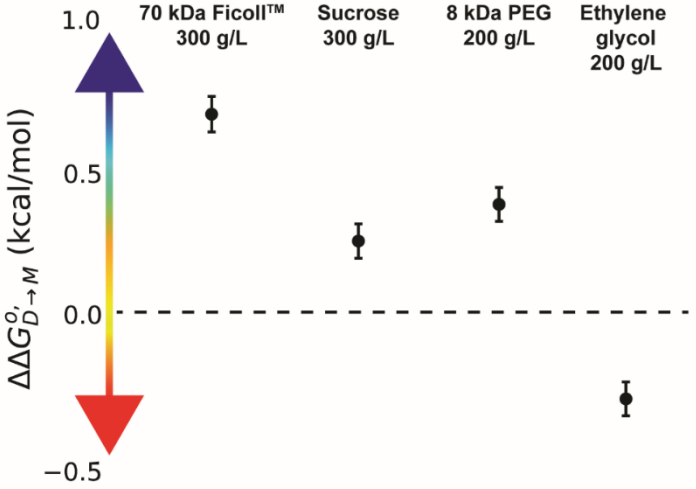

Figure 4: Free energy thermometer showing the effects of the hard-core repulsions probes on dimer stability. Error bars were calculated as the standard deviation from triplicate experiments.

Chemical interactions. We first tested dimer stability in two controls: 100 g/L urea and 38 g/L trimethylamine-*N*-oxide (TMAO). Urea was used since it is a protein denaturant from its high degree of backbone interactions.[16] As such, we expected it to favor the open, unstable monomer state, making it a good control for attractive chemical interactions. TMAO has the opposite effect of urea, in that it excludes backbone instead of interacting with it.[17] We expected it to favor the state with the most excluded

backbone, in that we expect it to favor the compact, structured dimer state, making it a good control for repulsive interactions. This was shown to be true, in that the addition of 100 g/L urea to the buffer led to a $K_{D\rightarrow M}$ of 840 ± 40 μM and the addition of 38 g/L TMAO to the buffer led to a $K_{D\rightarrow M}$ of 68 ± 4 μM.

Next, we were interested in picking an experimental cosolute to probe attractive interactions, and another that could probe repulsive interactions. This choice was made easier when we considered protein charge. At pH 7.5, the GB1 variant has a charge of -8.3. As such, we wanted to choose one protein which is positively charged at pH 7.5 for probing attractive interactions and another which is negatively charged at pH 7.5 for probing repulsive interactions. We chose lysozyme and BSA, which have charges of +7.1 and -37.9 at pH 7.5, respectively. The addition of 100 g/L BSA to buffer resulted in a $K_{D\rightarrow M}$ of 38 ± 3 μM and the addition of 50 g/L lysozyme to buffer resulted in a $K_{D\rightarrow M}$ of 110 ± 5 μM. A lower amount of lysozyme was added than that of BSA because the peaks were too broad to be analyzed at 100 g/L lysozyme. These data were used to calculate the $\Delta\Delta G'^{o}_{D\rightarrow M}$, and uncertainties were calculated as standard deviation of the mean from triplicate analysis. These results are summarized in figure 5.

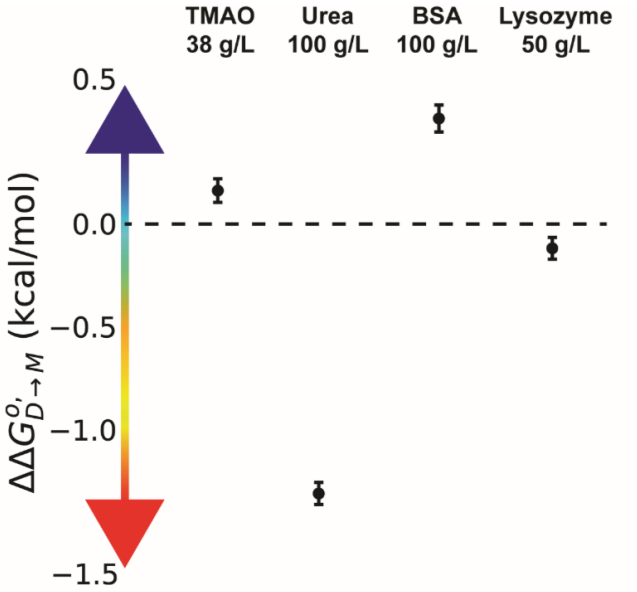

Figure 5: Free energy thermometer showing the effects of the chemical interactions probes on dimer stability. Error bars were calculated as the standard deviation from triplicate experiments.

The effects of polymer chain length. To test the effects of the molecular weight of the cosolute, we tested the stability of the domain swapped dimer in several different types of PEG. We used 20 kDa PEG and 3.35 kDa PEG to test the effects of decreasing and increasing the polymer molecular weight on dimer stability.

The concentration in buffer of the 3.35 kDa and 20 kDa PEG was 200 g/L. The 3.35 kDa PEG adjusted the stability by 0.08 kcal/mol, while the 20 kDa PEG adjusted the dimer stability by 0.37 kcal/mol. These results were compared with the 8 kDa PEG and ethylene glycol data in figure 6 and.

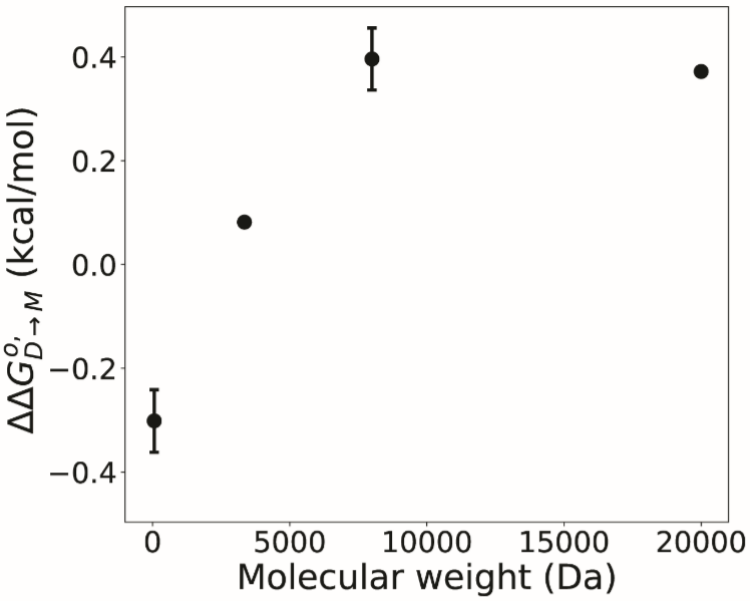

Figure 6: Plot of molecular weight versus $\Delta\Delta G^{o'}_{D\rightarrow M}$. Error was propagated as the standard deviation of the mean from triplicate experiments. Error bars are not shown for 3.35 kDa and 20 kDa PEG since experiments with those cosolutes have only been performed once.

Discussion

Domain swapped proteins vary greatly in function, with functions varying greatly from toxins to circadian clock regulators.[18,19] As such, it is of great importance to understand the effects of the cellular interior on dimers formed in this manner. We characterized the effects of many different cosolutes on the GB1 domain-swapped homodimer, and all facets of the data have yielded interesting results.

The synthetic polymer cosolutes used to generate hard-core repulsions led to stabilizing of the GB1 domain swapped homodimer. The addition of 200 g/L 8 kDa PEG led to a stabilization of the dimer by 0.39 ± 0.06 kcal/mol, and the addition of 300 g/L 70 kDa Ficoll led to a stabilization by 0.71 ± 0.06 kcal/mol. The monomers had a different or diminished effects than the polymers they constituted. Although 70 kDa Ficoll stabilized the dimer by 0.71 ± 0.06 kcal/mol, the sucrose monomer only stabilized the dimer by 0.26 ± 0.06 kcal/mol. Surprisingly, while 8 kDa PEG stabilized the dimer by 0.39 ± 0.06 kcal/mol, the ethylene glycol monomer destabilized the dimer by 0.30 ± 0.06 kcal/mol. The differences in the cosolute effect of the monomers and polymers suggest that upon formation of the polymer, changes occur in how the molecules interact with the protein. This is called the macromolecular effect, and has been previously observed with PPIs.[20,21] This best manifests itself in ethylene glycol and 8 kDa PEG. Ethylene glycol contains two hydroxyl groups (figure 7). These hydroxyl groups most likely have attractive chemical interactions with the protein surface. These attractive interactions are maximized in the monomer state since it has the most exposed surface area, pushing the equilibrium towards the monomer. Upon formation of the PEG polymer, many of these hydroxyl groups will become buried, and excluded volume will play a larger role as these groups become buried. Now, the more compact dimer state is favored.

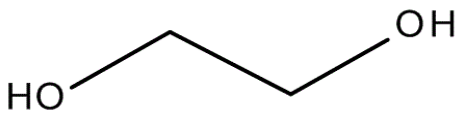

Figure 7: Structure of ethylene glycol

The macromolecular effect observed with the hard core repulsions experiments prompted us to carry out experiments to verify this observation. To do so, we carried out

the experiments with the different sizes of PEG. The data show more evidence for a macromolecular effect. The stability data from 3.35 kDa PEG fill the gap between ethylene glycol and 8 kDa PEG. Since the 3.35 kDa point lies between the 8 kDa PEG, this is more conclusive evidence that a macromolecular effect is present upon polymerization of the chain. With the effects that are observed, I hypothesize that the effects of PEG will approach ethylene glycol as the chain length is decreased.

These data are also interesting due to the 20 kDa point, in that there was not an increase in stability as the PEG lengthens from 8 kDa to 20 kDa. This inform us that the macromolecular effect present is saturable. Then, it also highlights some of the importance of chemical interactions. If the crowder were to be a hard, impenetrable sphere, we might expect that the protein would be more stable with a larger polymer. However, this is not what a true polymer acts as, since it will have chemical interactions with the test protein. Furthermore, we must also consider the polymer overlapping shown in Figure 3. Although I have not measured the overlap concentrations, others have measure the overlap concentrations of different PEGs. It was found that 6 kDa and 20 kDa PEG had a c^* of 119.2 and 50.9 g/L, respectively.[22] Since c^* is directly proportional to molecular weight[22], this tells us that at 200 g/L, we must be over the c^* concentration for 8 kDa and 20 kDa PEG. As such, we would want to carry out experiments below the *c** of the PEG crowders to better understand the effects of polymer overlap on protein stability.

Urea and TMAO had similar effects on PPIs as they do on protein folding.[5] Urea modulated dimer stability by -1.31 ± 0.05 kcal/mol, and TMAO modulated dimer stability by 0.16 ± 0.06 kcal/mol. The effects of the protein cosolutes varied based on the charge

of the protein cosolutes. BSA has a charge of -18 at a pH of 7.5, while lysozyme has a charge of +8 at a pH of 7.5. Lysozyme modulated dimer stability by -0.12 ± 0.05 kcal/mol. This destabilization arises due to the positive changes on the surface of lysozyme interacting with the negative charges on the surface of GB1 (figure 8). Since the monomeric species have more surface area available for interacting with the lysozyme, the monomer is favored. BSA has the opposite effect, where it modulates dimer stability by 0.51 ± 0.07 kcal/mol. Here, the negatively charged BSA has repulsive interactions with the negatively charged patches of GB1. To minimize these interactions, the dimer is favored since it has less exposed surface area than the individual monomers.

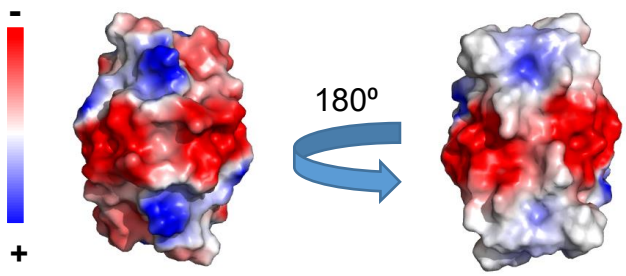

Figure 8: Electrostatic map of GB1 along with a diagram showing the meaning of each of the colors. Note the large acidic patches and basic patches on the surface.

Conclusions

Our study emphasizes the importance of macromolecular crowding on a domain-swapped homodimer. We used a variety of cosolutes to test the effects of hard-core repulsions and chemical interactions. We found that hard-core repulsions favored dimerization. The use of polymers and their monomers led to us observing a macromolecular effect. This result was supported by the experiments with differing molecular weights of PEG, where we found that there was evidence of a saturable macromolecular effect. Chemical interactions varied for each of the selected cosolutes,

but we found that repulsive interactions stabilized the dimer while attractive interactions destabilized the dimer. Due to the stark differences between the protein and polymer cosolutes, this work shows that polymer cosolutes are not good models of the cellular interior. The results of the macromolecular effect experiments are interesting in that they agree with past work showing similar effects for PPIs.[20,21] Those results also show a sharp dichotomy between protein folding and PPIs. With protein folding, it was found that monomers were more effective at stabilizing proteins than the polymers they make up[5], whereas it was found that polymers were more effective at stabilizing the dimer (figure 4). The future directions of this work could include sampling concentrations above and below the c^* of the polymers to better understand the effects of polymer overlap on dimer stability and also carrying out temperature experiments to calculate the enthalpic and entropic components of the modulation of dimer stability.[5]

Materials and Methods

Vector. A pET11a plasmid containing the GB1 A34F variant was used as the wild-type vector. Agilent's QuickChange mutagenesis kit was then used to induce the other mutations (L5V;F30V;Y33F) to make the domain-swapped homodimer variant.

Protein expression and purification. The plasmid encoding the GB1 mutant was transformed into competent BL21 (DE3) Gold *Escherichia coli* cells and spread onto LB-agar plates containing 100 µg/mL ampicillin. Following overnight incubation at 37 ºC, a single colony from the plates was used to inoculate a 25-mL overnight culture in LB containing 1 mM of ampicillin, and the culture was incubated overnight with shaking at

225 rpm at 37 ºC (New Brunswick Scientific, model I26). This overnight culture was used to inoculate a 975 mL culture in M9 minimal medium (50 mM Na2HPO4, 20 mM KH2PO4, 9 mM NaCl, 1 g/L NH4Cl, 4 g/L glucose, 2 mM MgSO4, 10 mg/mL thiamine HCl, 10 mg/mL biotin, 100 µM CaCl2, and 100 µg/mL ampicillin). The culture was grown with shaking at 37 ºC, and its optical density at 600 nm (OD_{600}) was monitored by UV-vis spectroscopy (Biorad Spectra Plus). Once an OD_{600} of 0.400 was reached, 500 mg of glyphosphate were added to inhibit aromatic amino acid synthesis, along with 60 mg of L-phenylalanine, 60 mg of L-tyrosine, and 70 mg of 5-fluoroindole. Once the culture reached an OD_{600} of 0.600, protein expression was induced by the addition of 1 mM isopropyl-β-D-thiogalactopyranoside. After 2 h, cells were harvested for 30 min at 4000 rpm (RC-3B Refrigerated Centrifuge; Sorvall Instruments).

Harvested cells were resuspended in 25 mL buffer A (20 mM Tris-HCl, pH 7.65), and 300 µL of protease inhibitor (Roche) were added prior to cell lysis. Cell lysis was carried out by sonication (Fischer Scientific Sonic Dismembrator model 500) using the following parameters: 15% amplitude, 0.50 s on, 0.50 s off, 20 min. The lysate was then spun down (RC-5B Refrigerated Superspeed Centrifuge; Sorvall Instruments) at 10,000 rpm for 1 h.

The supernatant was filtered through a 0.22-µm syringe-driven unit (Millex), and loaded onto an anion exchange column with Q Sepharose exchange resin (16 mm x 200 mm Q Sepharose; GE Healthcare) at 4 ºC on an AKTA Pure FPLC (GE Healthcare). Buffer A was used to equilibrate, load lysate, and elute impurities. Buffer B (20 mM Tris-HCl, 2 M NaCl at pH 7.65) was used to produce a linear gradient of 0-500 mM NaCl, which eluted the protein from the column. Eluate was assessed using SDS-

PAGE (4-20% Criterion TGX gels; Biorad) stained with Coomasie Brilliant Blue R-250. Fractions containing the GB1 mutant were concentrated using a 3000 Da MWCO centrifugal concentrator (Millipore). The concentrated sample was then filtered through a 0.22-µm syringe-driven unit (Millex), and loaded onto a size exclusion chromatography column (16 mm x 600 mm Superdex 75; GE Healthcare) at 4 ºC. The column was equilibrated with two column volumes of 5 mM Na2HPO4, 2 mM KH2PO4, 0.9 mM NaCl buffer at pH 7.5. The eluate was assessed again using SDS PAGE, and fractions containing the GB1 mutant were concentrated using a 3000 Da MWCO centrifugal concentrator (Millipore). The concentrated protein was then exchanged thrice into 18.00 MΩ deionized water. The protein concentration was measured using UV-vis spectrophotometry (NanoDrop One). An extinction coefficient at 280 nm of 8400 L M^{-1} cm^{-1} was used. The protein was split into 500 µM aliquots and lyophilized for 12-16 h (Labonco Freezone).

Crowder preparation. All crowders were dissolved in 20 mM sodium phosphate buffer, and the pH was adjusted to 7.5. For the preparation of protein cosolutes, lyophilized lysozyme and bovine serum albumin were purchased from Sigma-Aldrich. Concentration of the BSA and lysozyme solutions were monitored using using extinction coefficients at 280 nm of 6700 L mg^{-1} cm^{-1} and 26400 L mg^{-1} cm^{-1}, respectively**.**

Fluorine-19 NMR. Fluorinated protein was resuspended in buffer (with or without cosolutes) to a final concentration of 500 μM. Experiments were consucted using a bruker Avance III HD spectrometer operating at a 19F Larmor frequence of 470 MHz equipped with a cryogenic QCI probe with an H/F channel. Over at least 128 scans, 31047 points were collected with a delay of 2 s, an acquisition time of 1.4 s, an offset of

100 pm, and a sweep width of 100 ppm. Samples were composed of 10% D2O for locking.

***Data analysis*.** The NMR spectra were analyzed using Topspin3.5pI6. An exponential line broadening fucniton of 10 Hz was applied to each free induction decay prior to FT analysis. The monomer and dimer peaks were integrated, and the fraction dimer (F_d) was calculated as the ratio of the area of the dimer peak divided by the sum of the area under the dimer and monomer peaks. These data were fit to equation [1] using MATLAB (R2017A), where P_t is the total protein concentration and $K_{D->M}$ is the equilibrium constant for dissociation.[20]

$$F_d = \frac{4P_t + K_d - \sqrt{K_d^2 + *8P_tK_d}}{4P_t} \quad [1]$$

Acknowledgments

I would like to thank the Pielak lab for help on this project and past projects. I would like to thank Annelis Gorensek-benitez for training me in the basics of protein biochemistry and biophysics, and Alex Guseman for helping me along the way with this specific project. Dr. Gary Pielak, my faculty advisor, provided useful scientific discussion on this project and was a great mentor. I would also like to thank Dr. Gregory Young for NMR spectrometer maintenance and help in carrying out the NMR experiments. Lastly, I would like to thank my thesis committee for taking the time to carry out my thesis defense.

References

1. Rivas, G., Ferrone, F. & Herzfeld, J. Life in a crowded world. *EMBO Rep.* **5,** 23–27 (2004).

2. Sarkar, M., Li, C. & Pielak, G. J. Soft interactions and crowding. *Biophys. Rev.* **5,** 187–194 (2013).

3. Minton, A. P. Excluded volume as a determinant of protein structure and stability. *Biopolymers* **20,** 2093–2120 (1981).

4. Acosta, L. C., Goncalves, G. M. P., Pielak, G. J. & Annelise, H. Large cosolutes , small cosolutes and dihydrofolate reductase activity. *Protein Sci.* **26,** 2417–2425 (2017).

5. Gorensek-benitez, A. H., Smith, A. E., Stadmiller, S. S., Goncalves, G. M. P. & Pielak, G. J. Cosolutes, Crowding, and Protein Folding Kinetics. *J. Phys. Chem. B* **121,** 6527–6537 (2017).

6. Monteith, W. B., Cohen, R. D., Smith, A. E., Guzman-Cisneros, E. & Pielak, G. J. Quinary structure modulates protein stability in cells. *Proc. Natl. Acad. Sci. U. S. A.* **112,** 1739–1742 (2015).

7. Smith, A. E., Zhou, L. Z., Gorensek, A. H., Senske, M. & Pielak, G. J. In-cell thermodynamics and a new role for protein surfaces. *Proc. Natl. Acad. Sci. U. S. A.* **113,** 1725–1730 (2016).

8. Byeon, I. J. L., Louis, J. M. & Gronenborn, A. M. A protein contortionist: Core mutations of GB1 that induce dimerization and domain swapping. *J. Mol. Biol.*

333, 141–152 (2003).

9. Zimmerman, Steven B.; Trach, S. O. Estimation Of Macromolecule Concentration And Excluded Volume Effect For The Cytoplasm Of E.coli. *J. Mol. Biol.* **222,** 599–620 (1991).

10. Pérez-Bercoff, Å., McLysaght, A. & Conant, G. C. Patterns of indirect protein interactions suggest a spatial organization to metabolism. *Mol. Biosyst.* **7,** 3056 (2011).

11. Mondal, S. *et al.* Regulation of the actin cytoskeleton by an interaction of IQGAP related protein GAPA with Filamin and Cortexillin I. *PLoS One* **5,** (2010).

12. Gonzalez, M. W. & Kann, M. G. Chapter 4: Protein Interactions and Disease. *PLoS Comput. Biol.* **8,** (2012).

13. Chen, H., Viel, S., Ziarelli, F. & Peng, L. 19F NMR: a valuable tool for studying biological events. *Chem Soc Rev* **42,** 7971–7982 (2013).

14. Harper, D. B. & O'Hagan, D. The fluorinated natural products. *Nat. Prod. Rep.* **11,** 123–133 (1994).

15. M, R. & RH, C. *Polymer Physics*. (Oxford University Press, 2003).

16. Stumpe, M. C. & Grubmüller, H. Interaction of urea with amino acids: Implications for urea-induced protein denaturation. *J. Am. Chem. Soc.* **129,** 16126–16131 (2007).

17. Hu, C. Y., Lynch, G. C., Kokubo, H. & Montgomery Pettitt, B. Trimethylamine N-oxide influence on the backbone of proteins: An oligoglycine model. *Proteins*

Struct. Funct. Bioinforma. **78,** 695–704 (2010).

18. Bell, C. E. & Eisenberg, D. Crystal structure of diphtheria toxin bound to nicotinamide adenine dinucleotide. *Biochemistry* **35,** 1137–1149 (1996).

19. Ye, S., Vakonakis, I., Ioerger, T. R., LiWang, A. C. & Sacchettini, J. C. Crystal Structure of Circadian Clock Protein KaiA from Synechococcus elongatus. *J. Biol. Chem.* **279,** 20511–20518 (2004).

20. Guseman, A. J. & Pielak, G. J. Cosolute and Crowding Effects on a Side-By-Side Protein Dimer. *Biochemistry* **56,** 971–976 (2017).

21. Munari, F. *et al.* Identification of primary and secondary UBA footprints on the surface of ubiquitin in cell-mimicking crowded solution. *FEBS Lett.* **591,** 979–990 (2017).

22. Ziębacz, N., Wieczorek, S. A., Kalwarczyk, T., Fiałkowski, M. & Hołyst, R. Crossover regime for the diffusion of nanoparticles in polyethylene glycol solutions: influence of the depletion layer. *Soft Matter* **7,** 7181 (2011).